Electromagnetic surface modes in one-dimensional photonic crystals with dispersive metamaterials

Tong-Biao Wang, Cheng-Ping Yin, Wen-Yao Liang, Jian-Wen Dong, and He-Zhou Wang*

State Key Laboratory of Optoelectronic Materials and Technologies, Zhongshan (Sun Yat-Sen) University, Guangzhou 510275, China

**Corresponding author: stswhz@mail.sysu.edu.cn*

Received April 15, 2009; accepted June 13, 2009;
posted June 30, 2009 (Doc. ID 110044); published July 27, 2009

We study the electromagnetic surface modes supported by the interface between semi-infinite one-dimensional photonic crystals composed of dispersive metamaterials and a homogeneous medium in the presence of the cap layer. A new type of surface mode is found in such structure, and these surface modes can exhibit strong resonance at the first period of the photonic crystal. These resonant surface modes originate from the material dispersion. Another type of surface mode with structural resonance can appear in the thick cap layer. The influences of physical parameters of the structure on the surface modes have also been investigated. © 2009 Optical Society of America

OCIS codes: 160.3918, 240.6690, 230.4170.

1. INTRODUCTION

Metamaterials have attracted extensive attention in recent years because of their novel properties [1–6]. There are mainly two types of metamaterial: double negative (DNG) materials and single negative (SNG) materials. The DNG materials with both negative permittivity ($\epsilon<0$) and negative permeability ($\mu<0$) are also called negative refraction index materials (NIMs), which were first studied theoretically around 40 years ago by Veselago [1]. The NIMs possess striking electromagnetic properties in contrast with conventional positive refraction index materials (PIMs) such as inverse Doppler shift, backward-oriented Cerenkov radiation and power flow [1]. The SNG materials with $\epsilon<0$ ($\mu>0$) and $\mu<0$ ($\epsilon>0$) are called ϵ-negative (ENG) materials and μ-negative (MNG) materials, respectively. Compared with propagating modes in PIMs and NIMs, SNG materials are opaque and support only evanescent modes. How to construct these metamaterials was not known until recently due to the absence of naturally occurring materials with negative magnetic permeability. Plenty of research for realizing these materials experimentally in the microwave has been reported [2–4]. Now, these materials have been successfully manufactured in the visible [5,6]. These artificial materials have exhibited special characteristics in multilayered structures [7–10].

Surface modes are a special type of wave that are confined at the boundary between two different media [11,12]. The condition for the existence of surface modes at an interface is that one material has a negative dielectric constant, and the other medium is a pure dielectric. As is well known, the effective dielectric constant of photonic crystals (PCs) can be negative at some frequencies, so the surface mode can appear at the interface of PCs and homogeneous medium [13–21].

The surface electromagnetic (EM) modes that exist at the interface of PCs were studied theoretically and experimentally in recent years, and considerable progress has been made. The excitation of surface EM waves in one-dimensional (1D) photonic bandgap arrays was achieved experimentally [14]. The sensitivity of surface states to the stack sequence of 1D PCs was researched [15,16]. The surface modes in semi-infinite 1D PC with a thin nonlinear cap layer were studied in [17], and the authors found that the surface states were very sensitive to the nonlinearity of the cap layer on the surface [17]. The presence of metamaterials with constant permittivity and permeability in the photonic crystal structure can support the surface waves with a backward energy flow and allows a flexible control of dispersion properties of the surface modes [18,19]. The author in [20] has studied the coupling between guided modes and Bolch modes of EM surface waves of 1D multilayer stacks. Artigas and Torner proposed to use specially designed 2D PCs for observation of the so-called Dyakonov modes localized at the surface of the crystal [21,22]. Lossless interface modes at the boundary between two 1D periodic dielectric structures were investigated in [23]. However, to the best of our knowledge, the surface modes on 1D PCs composed of dispersive metamaterials has not been reported.

In this paper, we derived the dispersion relation of surface mode of 1D PCs with a cap layer by the transfer matrix method, which is different from the direct matching procedure within the Kronig–Penney model [19]. We have systematically studied the dependences of surface modes on the physical parameters of the structure. Two types of resonant surface modes are found in this semi-infinite 1D PC. The structural resonant surface modes appear in the thick cap layer at high frequency ranges, and the material strong resonant surface modes appear in the first period of the 1D PCs at low frequency ranges.

The organization of the paper is the following. In Section 2, we derived the dispersion relation of localized surface modes in a semi-infinite 1D PC with the cap layer. In

Section 3, we investigate the dependence of the surface modes on the stack sequence of the 1D PCs and the physical parameters of the cap layer. In Section 4, we present a brief summary to this paper.

2. THEORY MODEL

The structure of our problem is shown in Fig. 1. The left-hand side is a semi-infinite homogeneous medium; its permittivity and permeability are denoted by ϵ_0 and μ_0, respectively. The right-hand side is a semi-infinite 1D PC alternately stacked with materials A and B along the z axis, and C is the cap layer. d_i, ϵ_i, and μ_i $(i=A,B,C)$ are the thickness, permittivity, and permeability of layer i $(i=A,B,C)$, respectively.

We assume the z axis is along the normal to the interface, and the wave vector component parallel to the layers $k_\parallel$ is along the y axis. For the transverse electric (TE) wave, the electric field $\vec{E}$ is in the reverse direction of the y axis; and for the transverse magnetic (TM) wave, the magnetic field $\vec{H}$ is in the y direction. The electric and magnetic fields in any layers can be related by transfer matrix [8–10,24–26]

$$M_i(d_i)=\begin{pmatrix}\cos(k_i d_i) & -\dfrac{1}{\sigma_i}\sin(k_i d_i)\\ \sigma_i \sin(k_i d_i) & \cos(k_i d_i)\end{pmatrix},\quad (i=A,B,C), \tag{1}$$

where $k_i=(\omega^2\epsilon_i\mu_i/c^2-k_\parallel^2)^{1/2}$, $\sigma_i=k_i/\mu_i$ for the TE wave and $\sigma_i=k_i/\epsilon_i$ for the TM wave. c is the light speed in vacuum, ω is the angular frequency.

In order to obtain the surface modes in the structure of Fig. 1, we divide the structure into three parts in space:

(1) In the right-hand side 1D periodic structure, the propagating EM waves have the form of Bloch modes. The amplitude of the EM field at $z=0$ can be written as the following column vector:

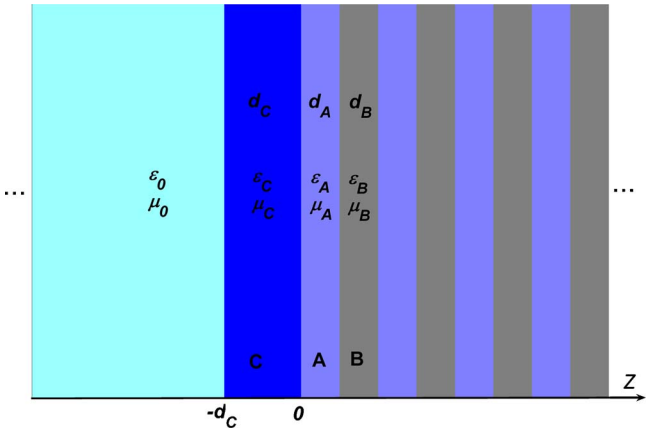

Fig. 1. (Color online) Schematic representation of the problem. The periodic structure is a semi-infinite 1D PC stacked with materials A and B; the left is a homogeneous medium, and C is the cap layer.

$$\begin{pmatrix}E_y(z)\\ jcH_x(z)\end{pmatrix}\Bigg|_{z=0}=\begin{pmatrix}M_{12}\\ e^{jKL}-M_{11}\end{pmatrix}, \tag{2}$$

where $j=\sqrt{-1}$, K is the Bloch wave vector, $L=d_A+d_B$ is the thickness of a unit cell, and M_{11} and M_{12} are the matrix components of the unit cell of the 1D PC.

(2) In the left-hand side semi-infinite homogeneous medium, the EM waves decay along the propagating distance. The vector of the EM field in this region has the following relationship:

$$\begin{pmatrix}E_y(z)\\ jcH_x(z)\end{pmatrix}\Bigg|_{z=-d_c}=\begin{pmatrix}Ce^{k_0 z}\\ -F_0 Ce^{k_0 z}\end{pmatrix}\Bigg|_{z=-d_c}, \tag{3}$$

where $F_0=k_0c/(\omega\mu_0)$, $k_0=(k_\parallel^2-\omega^2\epsilon_0\mu_0/c^2)^{1/2}$, and C is only a constant.

(3) Because the 1D PC and the homogeneous medium are connected by the cap layer in space, the EM field at the interface of the cap layer and the homogeneous medium is continuous; the EM field at the interface of the cap layer and the semi-infinite 1D PC is also continuous. The EM fields at the boundary of the right- and the left-side structures can be connected by the transfer matrix M_C, i.e.,

$$\begin{pmatrix}M_{12}\\ e^{jKL}-M_{11}\end{pmatrix}=M_C\begin{pmatrix}Ce^{k_0 z}\\ -F_0 Ce^{k_0 z}\end{pmatrix}\Bigg|_{z=-d_c}. \tag{4}$$

The dispersion relation of surface mode can be easily obtained with the help of Eq. (4). Thus,

$$\frac{M_{11}-e^{jKL}}{M_{12}}=\frac{\sigma_C(\sigma_C\sin(k_C d_C)-F_0\cos(k_C d_C))}{\sigma_C\cos(k_C d_C)+F_0\sin(k_C d_C)}. \tag{5}$$

We obtain the similar equation as that in [19]. The above method can be easily understood physically. This is a transcendent equation of frequency and parallel wave vector, which can be numerically solved. Equation (5) reduces to $M_{11}-e^{jKL}+F_0M_{12}=0$ when $d_C=0$, which has the same form as that in [15]. It is the special case of the one without the cap layer.

3. RESULTS AND DISCUSSION

Now, we consider the right-side semi-infinite 1D PC alternately stacked with two types of dispersive metamaterial. In this paper, the relative permittivity and permeability of metamaterial are given by the Drude model [8,27,28],

$$\epsilon_i=\epsilon_{0i}-\frac{\omega_{ep,i}^2}{\omega^2},\quad \mu_i=\mu_{0i}-\frac{\omega_{mp,i}^2}{\omega^2},\quad (i=A,B), \tag{6}$$

where ϵ_{0i} (μ_{0i}) and $\omega_{ep,i}$ $(\omega_{mp,i})$ are the effective static electric (magnetic) constants and the effective electric (magnetic) plasma frequencies, respectively. Here, we choose $\epsilon_{0i}=\mu_{0i}=2.828$, $(2\pi\omega_{ep,A}L/c)^2=(2\pi\omega_{mp,B}L/c)^2=428.8$, $(2\pi\omega_{mp,A}L/c)^2=(2\pi\omega_{ep,B}L/c)^2=73.6$. This model can be realized in artificial designed transmission lines [27,28]. For convenience, we substitute $\omega L/c$ with Ω as reduced frequency. Materials A and B can exhibit different properties in different frequency ranges from Eq. (6). Both materials A and B are PIMs when $\Omega>1.96$; both materials A

and B are NIMs when $\Omega<0.812$; when $0.812<\Omega<1.96$, A and B are ENG and MNG materials, respectively.

A. The Case of Semi-Infinite 1D PCs without the Cap Layer

First, we study the surface modes of this semi-infinite 1D PC adjacent to an air background in the absence of the cap layer. We study the surface modes of TE polarization only, and the surface modes of TM polarization can be obtained in a similar way. The projected band structure as well as the dispersion curves of the surface modes are displayed in Fig. 2. The thicknesses of materials A and B are $d_A=d_B=0.5L$. For convenience, we denote the structure of stack sequences of the semi-infinite 1D PC arrayed in the ABAB… and BABA… as samples I and II, and their surface modes are shown by dashed and dotted lines, respectively. In Fig. 2, there exist two complete bandgaps, which have been studied in [8]. One can see that the stack sequences of the semi-infinite 1D PC have a great influence on the surface modes. In sample I, the slope of the dispersion curves of the surface modes is positive, but in sample II, the slope of the dispersion curves can be both positive and negative. For sample II, most of the surface modes distribute in the low-frequency bandgaps.

We also study the electric fields of the surface modes of different samples in Fig. 3. Figures 3(a) and 3(b) are the electric fields of surface modes of sample I, and Figs. 3(c) and 3(d) are the electric fields of surface modes of sample II. The corresponding points of their modes are shown in Fig. 2. In Fig. 3(a), the electric field localized at the first layer of the 1D PC; it has decay behavior similar to the surface modes supported by conventional semi-infinite 1D PC [15,16]. In Fig. 3(b), materials A and B are ENG and MNG, respectively. The electric field localized at the interface of the homogeneous medium and the semi-infinite 1D PC, and it exhibits different decay behavior compared to that in Fig. 3(a) because of the interaction of evanescent wave tunneling. Figure 3(c) is similar to Fig. 3(a). In Fig. 3(d), the electric field forms a standing wave in each cell of the semi-infinite 1D PC. But the standing wave is apparent only in the first period of the 1D PC because of the quick decay. Mode (d) is a strong resonant surface mode, which we will discuss at the end of Section 3.

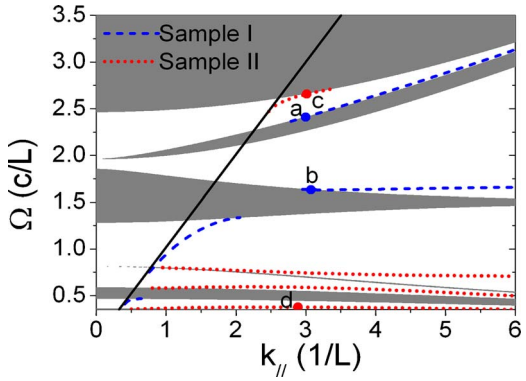

Fig. 2. (Color online) Calculated surface modes for TE polarization in a semi-infinite 1D PC composed of metamaterials without the cap layer. The parameters of the structure are $d_A=d_B=0.5L$. The dashed lines and dotted lines are the surface modes of samples I and II, respectively. The solid line is the light line of air.

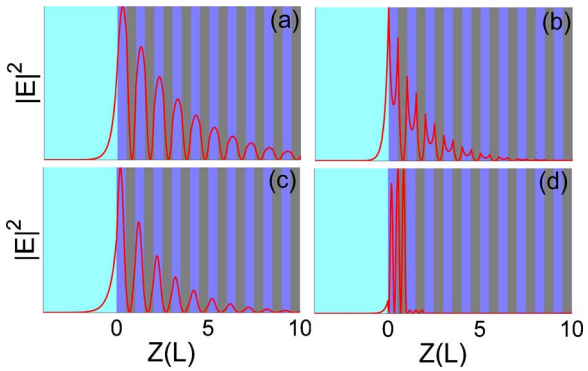

Fig. 3. (Color online) The electric field distributions of surface modes of the structure without cap layer. (a) $\Omega=2.41$, $k_{\|}=2.9988$; (b) $\Omega=1.632$, $k_{\|}=3.0758$; (c) $\Omega=2.6570$, $k_{\|}=3.0142$; (d) $\Omega=0.3765$, $k_{\|}=2.8896$.

In Fig. 2, we studied only the case in which the thicknesses of materials A and B are the same. As is well known, the thickness ratio of constituents in 1D PCs has a great impact on the photonic bandgaps. Therefore, the surface modes can also be affected by the thickness ratio of constituents. In order to show the dependence of the surface modes on the ratio of the thicknesses of two media in the semi-infinite 1D PC without the cap layer, we plot the surface modes as a function of the ratio d_A/L at $k_{\|}=3.0$ in Fig. 4. The ratio varies from 0.1 to 0.9. There are more surface modes apparent in the bandgaps compared to the case when $d_A/L=0.5$. The slope of the dispersion curves of surface modes of samples I and II can exhibit both positive and negative properties as the ratio increase. Most of the surface modes of sample II still concentrate on lower frequency ranges.

B. The Case of Semi-Infinite 1D PCs with the Cap Layer

Generally speaking, the cap layer usually plays an important role in studying the surface modes. So it is interesting in the study of the dependence of surface modes on physical parameters of the cap layer. Here, we employ conventional PIM as the cap layer. In Fig. 5, we plot the surface modes of the semi-infinite 1D PC with a cap layer whose physical parameters are $d_C=0.5L$, $\epsilon_C=4.0$, and $\mu_C=1.0$. More surface modes appear in this case compared with the case without the cap layer. The dispersion curves of the surface modes of sample I have positive slope; and

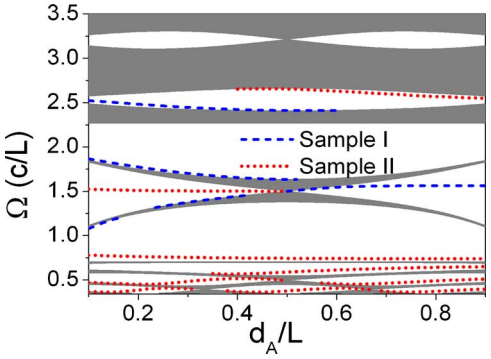

Fig. 4. (Color online) The surface modes as a function of d_A/L at $k_{\|}=3.0$ without the cap layer. The dashed lines and dotted lines are the surface modes of samples I and II, respectively.

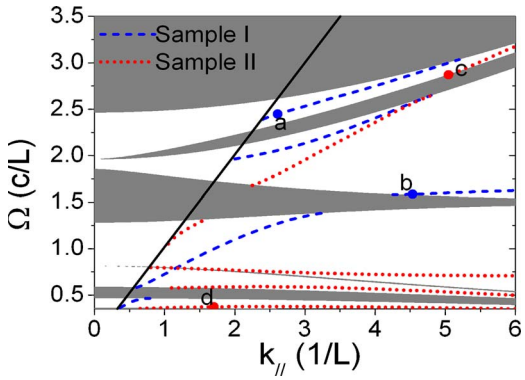

Fig. 5. (Color online) Surface modes of 1D PC composed of metamaterials with a PIM cap layer. The parameters of the structure are $d_A=d_B=0.5L$, $d_C=0.5L$, $\epsilon_C=4.0$, $\mu_C=1.0$. The dashed lines and dotted lines are the surface modes of samples I and II, respectively. The solid line is the light line of air.

the dispersion curves of the surface modes of sample II can exhibit positive slope when $\Omega>1.0$, and they exhibit negative slope when $\Omega<1.0$. For sample II, the surface modes in lower frequencies do not vary much in contrast with the case without the cap layer, that is to say, the surface modes of sample II are not sensitive to the cap layer in the lower frequency ranges.

We display the electric fields of the surface modes of the semi-infinite 1D PC with the cap layer in Fig. 6. Modes (a), (b), (c), and (d) correspond to the points in Fig. 5. In Fig. 6(a), the electric field localized at the interface of the first and second layer of the semi-infinite periodic structure. The electric field decays to zero at the interface of the semi-infinite periodic structure and the cap layer, and it increases from zero to submaximum at the interface of the cap layer and the homogeneous medium. In Fig. 6(b), the electric field localized at the interface of the cap layer and the semi-infinite periodic structure, the electric field decays quickly. Figure 6(b) has similar decay behavior as Fig. 3(b). In Fig. 6(c), the electric field decays fast into the cap layer and decays slowly in the semi-infinite periodic structure. In Fig. 6(d), the electric field forms a standing wave in the first period of semi-infinite periodic structure and decays quickly to zero in two directions. Mode (d) is also a resonant surface mode.

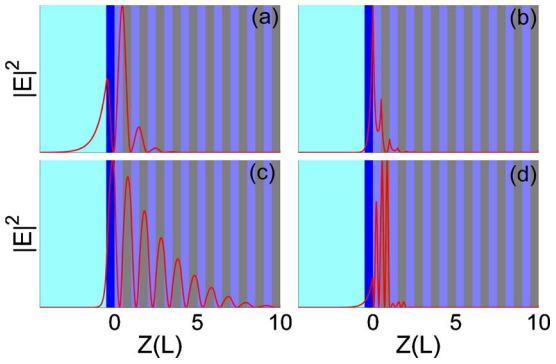

Fig. 6. (Color online) The electric field distributions of surface modes of the structure with a PIM cap layer. The parameters of the cap layer are the same as that in Fig. 5. (a) $\Omega=2.447$, $k_{\|}=2.613$; (b) $\Omega=1.584$, $k_{\|}=4.536$; (c) $\Omega=2.8696$, $k_{\|}=5.0490$; (d) $\Omega=0.3732$, $k_{\|}=1.7040$.

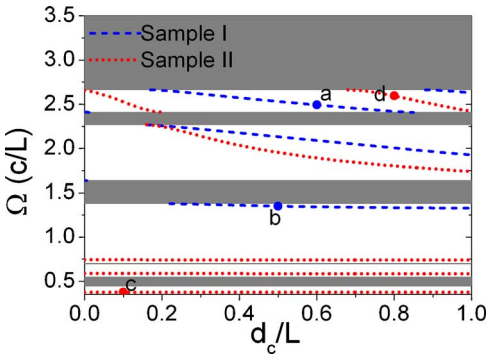

Fig. 7. (Color online) Surface modes of semi-infinite 1D PC composed of metamaterials as a function of the thickness of the cap layer at $k_{\|}=3.0$, $\epsilon_C=4.0$. The dashed lines and dotted lines are the surface modes of samples I and II, respectively.

In the following, we study the influence of the thickness of the cap layer on the surface modes with parameters $\epsilon_C=4.0$ and $\mu_C=1.0$. The thickness of the cap layer d_C varies from 0 to $1.0L$. Figure 7 is plotted to show the surface modes as a function of d_C/L at $k_{\|}=3.0$. The surface modes move from the upper band edges to low band edges as d_C/L increase for both samples I and II when $\Omega>1.0$. But in the lower frequencies ($\Omega<1.0$), the dispersion curves of surface modes of sample II are almost invariable. The electric fields of these four modes in Fig. 7, marked as (a), (b), (c), and (d), are plotted in Fig. 8. The electric field localized at the interface of the first layer and second layer of the periodic structure in Fig. 8(a). It has property similar to that of mode (a) in Fig. 6. In Fig. 8(b), the electric field localized at the interface of the cap layer and the 1D PC, and quickly decays to the right and left side of the total structure. The electric field in Fig. 8(c) has property similar to that in Fig. 6(d). In Fig. 8(d), the electric field reaches maximum at the interface of the semi-infinite periodic structure and it the cap layer, and it decays to zero in the cap layer and becomes submaximum at the interface of the cap layer and the homogeneous medium.

Finally, we investigate the influence of the permittivity of the cap layer to the surface modes with the parameters are $d_C=1.0L$ and $\mu_C=1.0$. The permittivity ϵ_C varies from 1.0 to 6.0. The surface modes of both samples I and II are shown in Fig. 9. The dispersion curves of the surface modes move to lower frequencies as ϵ_C increase when $\Omega>1.0$; and the dispersion curves of surface modes of

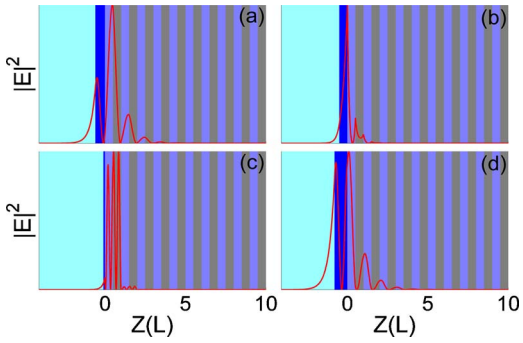

Fig. 8. (Color online) The electric field distributions of surface modes of the structure with a PIM cap layer. The parameters are the same as that in Fig. 7. (a) $d_C=0.6L$, $\Omega=2.4924$; (b) $d_C=0.5L$, $\Omega=1.3497$; (c) $d_C=0.1L$, $\Omega=0.3761$; (d) $d_C=0.8L$, $\Omega=2.5958$.

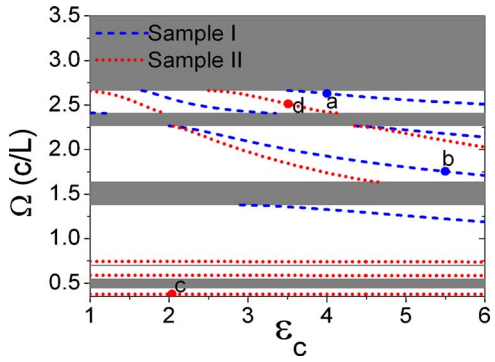

Fig. 9. (Color online) Surface modes of 1D PC composed of metamaterials as a function of the permittivity of the cap layer at $k_{\|}=3.0$, $d_C=1.0L$. The dashed lines and dotted lines are the surface modes of samples I and II, respectively.

sample II are also almost invariable when $\Omega<1.0$, which exhibits the property similar to that in Fig. 7. The electric fields of four modes in Fig. 9, marked as (a), (b), (c), and (d), are plotted in Fig. 10. In Fig. 10(a), the electric field localized at the interface of the first and second layers of semi-infinite 1D PC. There is a standing wave with smaller strength in the cap layer. The electric field localized at the cap layer in Fig. 10(b) and decays quickly in both directions of the total structure. In Fig. 10(c), a standing wave appears in the first period of the semi-infinite 1D PC, and the electric field decays quickly to the cap layer and the semi-infinite periodic structure. In Fig. 10(d), the electric field localized in the cap layer and forms a standing wave.

At the end of this paper, we discuss the physics mechanism of these surface modes. At the lower frequency ranges, both materials A and B are NIMs with a very-high negative refraction index. The difference of the refraction index between the materials of 1D PC and the cap layer or homogeneous medium is great. The EM waves can be strongly reflected at the interface between the semi-infinite 1D PC and its adjacent material. So the strong resonant surface modes exist at the first period of the semi-infinite 1D PC, and it appears in the form of standing wave, such as Fig. 3(d), Fig. 6(d), Fig. 8(c), and Fig. 10(c). Because these surface modes mainly originate from material dispersion, they can be called material resonant surface modes. In the higher frequency ranges, both materials A and B are PIMs, and the surface modes supported by PIMs have been extensively studied. When the thickness of the cap layer is increasing, the total structure can be treated as a dielectric waveguide, which is with the cap layer as the core surrounded by the homogeneous medium on one side and by the semi-infinite 1D PC on the other side. In this case, the surface modes behave more like a guided mode. The electric fields of the surface modes form standing waves in the cap layer with a thicker width because of the cavity resonance such as in Figs. 10(a) and 10(d). These modes can be called structural resonant surface modes. But for a thin cap layer, the cavity resonance can't occur [such as in Fig. 6(a), Fig. 6(c), and Fig. 8(a)]. In the middle frequency ranges, materials A and B are ENG and MNG materials, respectively. The photonic crystals composed of ENG and MNG materials can support only evanescent waves. The electric fields show different characteristics due to the interaction of the evanescent waves, such as in Fig. 3(b), Fig. 6(b), Fig. 8(b), and Fig. 10(b). Although the cap layer is thick, the resonance can't appear in this case, e.g., see Fig. 10(b).

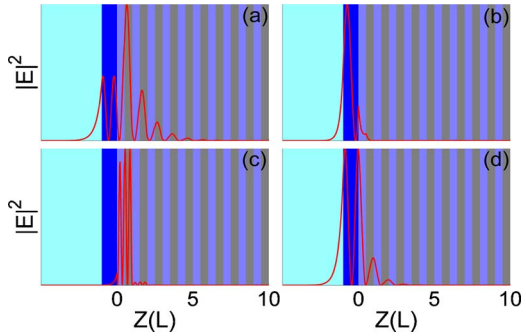

Fig. 10. (Color online) The electric field distributions of surface modes of the structure with a PIM cap layer. The parameters are the same as that in Fig. 9. (a) $\epsilon_C=4.0$, $\Omega=2.6295$; (b) $\epsilon_C=5.5$, $\Omega=1.7543$; (c) $\epsilon_C=2.04$, $\Omega=0.3761$; (d) $\epsilon_C=3.51$, $\Omega=2.5114$.

4. CONCLUSION

In conclusion, we have studied the electromagnetic surface modes guided by an interface between a homogenous medium and semi-infinite one-dimensional photonic crystals composed of dispersive metamaterials. We have derived the dispersion relation of the surface mode in the presence of the cap layer with the help of the transfer matrix method. The surface modes strongly depend on the stack sequence of the semi-infinite 1D PC. The dependence of the surface modes on the cap layer has also been investigated in detail. Two types of resonant surface modes can exist in different frequency ranges. The material resonant surface modes localized in the first period of the photonic crystal are not sensitive to the cap layer, while the structural resonant surface modes only appear for a thick cap layer in high frequency ranges. We believe that these novel results will be useful for studying metamaterials and surface modes.

ACKNOWLEDGMENTS

This work is supported by the National Natural Science Foundation of China (NSFC) (10874250, 10674183, 10804131), National 973 Project of China (2004CB719804), and Ph. D Degrees Foundation of Education Ministry of China (20060558068).

REFERENCES

1. V. G. Veselago, "The electrodynamics of substances with simultaneously negative values of ϵ and μ," Sov. Phys. Usp. **10**, 509–514 (1968).
2. D. R. Smith, W. J. Padilla, D. C. Vier, S. C. Nemat-Nasser, and S. Schultz, "Composite medium with simultaneously negative permeability and permittivity," Phys. Rev. Lett. **84**, 4184–4187 (2000).
3. R. A. Shelby, D. R. Smith, and S. Schultz, "Experimental verification of a negative index of refraction," Science **292**, 77–79 (2001).
4. J. B. Pendry, A. J. Holden, W. J. Stewart, and I. Youngs, "Extremely low frequency plasmons in metallic mesostructures," Phys. Rev. Lett. **76**, 4773–4776 (1996).

5. G. Dolling, C. Enkrich, M. Wegener, C. M. Soukoulis, and S. Linden, "Negative-index metamaterial at 780 nm wavelength," Opt. Lett. **32**, 53–55 (2007).
6. U. K. Chettiar, A. V. Kildishev, H. K. Yuan, W. Cai, S. Xiao, V. P. Drachev, and V. M. Shalaev, "Dual-band negative index metamaterial: double negative at 813 nm and single negative at 772 nm," Opt. Lett. **32**, 1671–1673 (2007).
7. J. Li, L. Zhou, C. T. Chan, and P. Sheng, "Photonic band gap from a stack of positive and negative index materials," Phys. Rev. Lett. **90**, 083901 (2003).
8. H. T. Jiang, H. Chen, H. Q. Li, Y. W. Zhang, and S. Y. Zhu, "Omnidirectional gap and defect mode of one-dimensional photonic crystals containing negative-index materials," Appl. Phys. Lett. **83**, 5386–5388 (2003).
9. L. G. Wang, H. Chen, and S. Y. Zhu, "Omnidirectional gap and defect mode of one-dimensional photonic crystals with single-negative materials," Phys. Rev. B **70**, 245102 (2004).
10. T. B. Wang, J. W. Dong, C. P. Yin, and H. Z. Wang, "Complete evanescent tunneling gaps in one-dimensional photonic crystals," Phys. Lett. A **373**, 169–172 (2008).
11. P. Yeh, A. Yariv, and C. S. Hong, "Electromagnetic propagation in periodic stratified media. I. General theory," J. Opt. Soc. Am. **67**, 423–438 (1977).
12. P. Yeh, A. Yariv, and A. Y. Cho, "Optical surface waves in periodic layered media," Appl. Phys. Lett. **32**, 104–105 (1978).
13. E. H. El Boudouti, B. Djafari-Rouhani, A. Akjouj, and L. Dobrzynski, "Theory of surface and interface transverse elastic waves in N-layer superlattices," Phys. Rev. B **54**, 14728–14741 (1996).
14. W. M. Robertson and M. S. May, "Surface electromagnetic wave excitation on one-dimensional photonic band-gap arrays," Appl. Phys. Lett. **74**, 1800–1802 (1999).
15. S. Feng, H. Sang, Z. Li, B. Cheng, and D. Zhang, "Sensitivity of surface states to the stack sequence of one-dimensional photonic crystals," J. Opt. A, Pure Appl. Opt. **7**, 374–381 (2005).
16. Y. El Hassouani, E. H. El Boudouti, H. Aynaou, B. Djafari-Rouhani, and V. R. Velasco, "Comment on 'Sensitivity of surface states to the stack sequence of one-dimensional photonic crystals'," J. Opt. A, Pure Appl. Opt. **9**, 308–313 (2007).
17. M. Kalafi, A. Soltani-Vala, and J. Barvestani, "Surface optical waves in semi-infinite one-dimensional photonic crystals with a thin nonlinear cap layer," Opt. Commun. **272**, 403–406 (2007).
18. A. Namdar, I. Shadrivov, and Y. Kivshar, "Backward Tamm states in left-handed metamaterials," Appl. Phys. Lett. **89**, 114104 (2006).
19. J. Barvestani, M. Kalafi, A. Soltani-Vala, and A. Namdar, "Backward surface electromagnetic waves in semi-infinite one-dimensional photonic crystals containing left-handed materials," Phys. Rev. A **77**, 013805 (2008).
20. C. Vandenbem, "Electromagnetic surface waves of multilayer stacks: coupling between guided modes and Bloch modes," Opt. Lett. **33**, 2260–2262 (2008).
21. M. I. D'yakonov, "New type of electromagnetic wave propagating at an interface," Sov. Phys. JETP **67**, 714–716 (1988).
22. D. Artigas and L. Torner, "Dyakonov surface waves in photonic metamaterials," Phys. Rev. Lett. **94**, 013901 (2005).
23. A. V. Kavokin, I. A. Shelykh, and G. Malpuech, "Lossless interface modes at the boundary between two periodic dielectric structures," Phys. Rev. B **72**, 233102 (2005).
24. C. Yeh and G. Lindgren, "Computing the propagation characteristics of radially stratified fibers: an efficient method," Appl. Opt. **16**, 483–493 (1977).
25. N. H. Liu, S. Y. Zhu, H. Chen, and X. Wu, "Superluminal pulse propagation through one-dimensional photonic crystals with a dispersive defect," Phys. Rev. E **65**, 046607 (2002).
26. C. Yeh and F. Shimabukuro, *The Essence of Dielectric Waveguides* (Springer, 2008).
27. J. W. Dong and H. Z. Wang, "Slow electromagnetic propagation with low group velocity dispersion in an all-metamaterial-based waveguide," Appl. Phys. Lett. **91**, 111909 (2007).
28. A. Alú and N. Engheta, "Pairing an epsilon-negative slab with a μ-negative slab: resonance, tunneling and transparency," IEEE Trans. Antennas Propag. **51**, 2558–2571 (2003).